Experimental enhancement of a CO_2 transcritical refrigerating plant including thermoelectric subcooling

D. Sánchez [a*], P. Aranguren [b], A. Casi [b], R. Llopis [a], R. Cabello [a], D. Astrain [b]

[a]Jaume I University, Dep. of Mechanical Engineering and Construction, Campus de Riu Sec s/n
E-12071, Castellón, Spain
[b]Public University of Navarra, Dep. of Engineering, Campus de Arrosadía s/n
E-31006, Pamplona, Spain

*Corresponding author: sanchezd@uji.es Tel.: +34 964 728142; Fax.: +34 964 728106

ABSTRACT

CO_2 is an excellent natural refrigerant that can be used in almost any commercial cooling application thanks to its useful range of evaporative temperatures and excellent environmental properties. However, due to its low critical temperature, CO_2 has an important issue related to the low performance of the simplest transcritical refrigeration cycle. To overcome it, the subcooling technique is a well-known method to improve the energy performance of any refrigeration cycle especially the CO_2 transcritical one. The IHX is a widely used example of this method that is implemented in almost all standalone systems that use CO_2 as a refrigerant. As an alternative of this element, in this work, a thermoelectric subcooling system is presented and tested in a CO_2 transcritical refrigerating plant. The experimental tests have been performed at two ambient temperatures: 25 and 30ºC, maintaining a constant evaporating level at -10ºC and varying the voltage supply to thermoelectric modules and the heat rejection pressure. The results from these experimental tests revealed that the COP and the cooling capacity of the refrigerating plant can be enhanced up to 9.9% and 16.0%, respectively, operating at the optimum operating conditions. Moreover, the experimental tests corroborate the existence of an optimum voltage which maximizes the COP, and the almost linear capacity regulation easily adjustable by varying the voltage supply.

KEYWORDS

CO_2, R744, subcooling, thermoelectric subcooling, transcritical cycle, IHX

HIGHLIGHTS

- A novel thermoelectric subcooler system has been experimentally analysed.
- Experimental tests are performed at -10ºC and two ambient temperatures: 25 and 30ºC.
- At the optimum conditions the TESC allows increasing the capacity up to 16.0%.
- At the optimum conditions the TESC allows increasing the COP up to 9.9%.
- Tests demonstrate the existence of an optimum voltage supply that maximizes COP.

Nomenclature

COP	coefficient of performance
c_P	specific heat at constant pressure ($kJ \cdot kg^{-1} \cdot °C^{-1}$)
DMS	dedicated mechanical subcooling
h	enthalpy per unit of mass ($kJ \cdot kg^{-1}$)
IHX	internal heat exchanger
$\dot{m}$	mass flow rate ($kg \cdot s^{-1}$)
P	pressure (bar)
$\dot{Q}$	heat transfer rate (W)
RH	relative humidity
SH	useful superheating (K)
T	temperature (°C)
V	voltage of TEMs (VDC)
$\dot{W}$	power input (W)

Greek Symbols

Δ	variation (increment or decrement)

Subscripts

amb	ambient
BP	back-pressure
CO_2	transcritical base cycle
FAN	heat-sink fan
GC	gas-cooler
glyc	mixture water and propylene-glycol
in	inlet / inner
LR	liquid receiver
O	evaporator
opt	optimum
out	out / outlet
plant	refrigerating plant
pseudo	pseudo critical temperature
SUB	subcooling degree
TEM	thermoelectric modules
TESC	thermoelectric subcooler

1. Introduction

The International Institute of Refrigeration (IIR) states that Refrigeration and heat, ventilation and air conditioning (HVAC) are responsible for the 7.8% of global greenhouse emissions, a total of 2.61 Gt of equivalent CO_2 [1]. The effect of a refrigeration system on the global warming is determined by the Total Equivalent Warming Impact (TEWI), which includes two terms: the indirect effect, that is, the impact of the energy consumption of the systems, and the direct effect, that includes the release of refrigerant into the atmosphere. The energy consumption of refrigeration and HVAC sectors accounted for the 17% of the electric energy consumption worldwide in 2014 [2], in this regard, into the refrigeration sector, the 63% of TEWI corresponds to the indirect effect (the energy consumption), while the remaining 37% to the usage of refrigerants, a non-negligible figure. Therefore, it is not only important to develop more efficient installations increasing their coefficient of Performance (COP), but also is essential to use refrigerants with lower impact on the environment. To that purpose, the research on refrigeration systems based on natural fluids with extremely low Global Warming Potential (GWP) is of paramount importance. Among these new refrigerants, CO_2 is considered as one of the most promising refrigerants due to its zero Ozone Depletion Potential (ODP), negligible GWP, non-flammability, non-toxicity, low cost and high availability [3-5].

Due to the low critical temperature of carbon dioxide (30.98ºC), CO_2 refrigeration systems normally operate in transcritical conditions, unlike conventional refrigerants. This new arrangement has important exergy losses that penalize the COP of the system [6,7]. Consequently, in the last years, several new elements have emerged to increase the COP of CO_2 basic units, such as Internal Heat Exchangers (IHX) [8,9], parallel compressors [10], combination of gas ejectors and parallel compressors [11], expanders [12], subcoolers [13,14] or multi-stage compression arrangements [15], among others. Nevertheless, the use of the previously presented systems is determined by the size of the refrigeration facility due to their costs and complexity. Only in the case of IHX, its use can be always adopted due to its low-cost.

The use of thermoelectric coolers to provide subcooling to a CO_2 transcritical refrigeration unit has been presented as an alternative to boost the COP of these systems. Thermoelectric refrigeration is based on the Peltier effect, which explains the direct conversion of electric power into cooling and heating powers [16]. A thermoelectric subcooler (TESC) is composed of thermoelectric modules (TEMs), solid-state heat engines that use electrons as the working fluid, so neither moving parts nor fluids are needed. Thus, the advantages that thermoelectric devices present, such as simplicity, robustness, compactness, absence of noise, durability and modularity, are deterrent to be included into transcritical CO_2 refrigeration systems to increase their COP, decrease their discharge pressures and increase the cooling power of these systems [17-23].

During the last years several computational studies have been published obtaining promising improvements on the transcritical cycle operation. Jamali *et al.* obtained a COP increment of the 3.4% using a two-stage

TESC [17]; Dai *et al.* reported an increment of the 22.5% on the COP and reductions in the discharge pressure of 15.3 bar [18]; Winkler *et al.* showed that when a thermoelectric device is used as a dedicated subcooler at the gas-cooler outlet of a transcritical CO_2 system, a 16.2% increase in system COP and over a 20% increase in cooling capacity can be achieved [19]; Sarkar *et al.* conducted a computational COP optimization varying the thermoelectric cooler current supply, the discharge pressure and the CO_2 subcooling obtaining an increase of the 25.6% on the COP and a reduction of the 15.4% of the discharge pressure [20]; finally, Astrain *et al.* revealed that a 20% increase on the COP and a 26.5% increase on the cooling capacity could be obtained including 20 TEMs at the gas-cooler outlet by optimizing the discharge pressure and the voltage supplied to the TEMs [21].

Although computational results are very positive and show a strong COP improvement when a TESC is added to the gas-cooler outlet, experimental studies that analyse this configuration are scarce. Schoenfeld *et al.* integrated a thermoelectric subcooler in a transcritical CO_2 facility made of 10 TEMs, a single aluminium microchannel CO_2 heat exchanger and a thermosyphon loop to release the heat. This facility was tested and a maximum COP improvement of the 5.2% was obtained while a maximum increment on the cooling capacity of the 15.3% was achieved at a different scenario [22]. Including further thermal optimization of the TESC, Schoenfeld obtained experimental increments on the COP of the transcritical CO_2 refrigeration system of the 10% while at this working point an increment of the cooling capacity of the 13% was obtained [23]. The latter optimization shows the importance of optimizing the thermal design and the assembly of the TESC to achieve higher global improvements, as many authors have stated before [24-27].

In view of the results published, the TESC is a very promising system to enhance the COP and the cooling capacity of transcritical cycles used in low-medium capacities units. However, there is an important lack of experimental assessments that corroborate the computational studies previously reported. Accordingly, this work presents an experimental assessment of using a TESC system in a CO_2 transcritical refrigeration plant at different operating conditions. The thermoelectric subcooler was installed at the exit of the gas-cooler and tested at two ambient temperatures: 25 and 30ºC and maintaining an evaporative level of -10ºC typically used in commercial refrigeration. The heat rejection pressure and the voltage supplied to the TEMs were varied as key parameters to maximize the COP of the refrigeration system under these operating conditions. The results obtained with the thermoelectric subcooler have been compared with those operating without subcooling giving substantial improvements of COP and cooling capacity at the optimum operating conditions.

2. Theoretical approach

Subcooling systems are usually installed at the exit of the gas-cooler to increase the specific capacity of the evaporator and the cooling capacity of the whole refrigerating plant. However, the positive effect of these

methods on the overall COP of the facility depends on the performance of the subcooling system itself. Focused on the thermoelectric subcooler system, Figure 1 presents a schematic of the refrigeration facility equipped with a TESC and its P-h diagram including the subcooling effect. The subscript CO_2 refers to the transcritical cycle while *TESC* is related to the thermoelectric subcooling system.

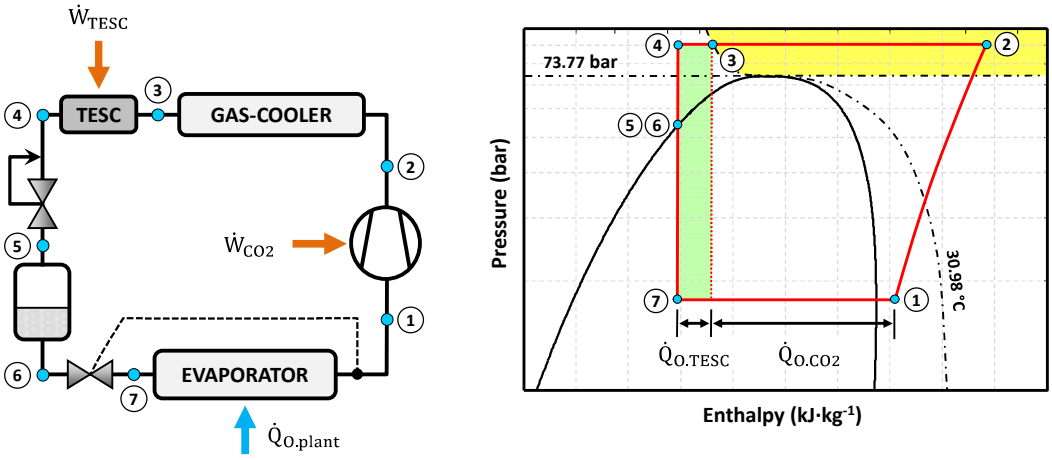

Figure 1 – CO_2 transcritical base cycle with thermoelectric subcooling system (left) and its P-h diagram (right)

From Figure 1, it is easy seeing that the cooling capacity of the entire refrigerating plant can be expressed as a sum of the cooling capacity of the base cycle ($\dot{Q}_{O,CO2}$) and the cooling effect introduced by the thermoelectric subcooling system ($\dot{Q}_{O,TESC}$) (Eq. 1). Thus, the effect of the TESC will be always positive in terms of cooling capacity and it will help the base cycle to improve its capacity.

$$\dot{Q}_{O.plant} = \dot{Q}_{O.CO2} + \dot{Q}_{O.TESC} \quad (1)$$

Regarding the power consumption of the refrigerating plant, it contains the electrical power consumption of the compressor ($\dot{W}_{CO2}$) and the power consumed by the TESC system ($\dot{W}_{TESC}$) that refers to the consumption of the thermoelectric modules and the auxiliary systems, such as fans (Eq. 2). Accordingly, the global power consumption of the refrigeration plant will be always higher than the base cycle.

$$\dot{W}_{plant} = \dot{W}_{CO2} + \dot{W}_{TESC} \quad (2)$$

The combination of both opposing effects can be obtained easily with Eq. 3 by using the coefficient of performance (COP_{plant}), which value will be greater than the base cycle (COP_{CO2}) if the condition $COP_{TESC} > COP_{CO2}$ is achieved (Eq. 4) [28].

$$COP_{plant} = \frac{\dot{Q}_{O.plant}}{\dot{W}_{plant}} \quad (3)$$

$$COP_{plant} > COP_{CO2} \rightarrow \frac{\dot{Q}_{O.CO2} + \dot{Q}_{O.TESC}}{\dot{W}_{CO2} + \dot{W}_{TESC}} > \frac{\dot{Q}_{O.CO2}}{\dot{W}_{CO2}} \rightarrow COP_{TESC} > COP_{CO2} \quad (4)$$

Taking into account this consideration, it is mandatory to determine how Eq. 4 can be achieved at specific operating conditions by varying the key parameters of the heat rejection pressure, that allows modifying the COP_{CO2}, and the voltage supplied of TEMs, which affects the COP_{TESC}. Accordingly, the following section experimentally analyses the effect of both parameters to determine the optimum operating conditions that allow maximizing the performance of the refrigerating plant (COP_{plant}).

3. Experimental test bench

3.1 Refrigeration facility

The refrigeration facility used to evaluate the performance of thermoelectric subcooling is a low-medium capacity system based on a one-stage transcritical cycle which schematic is presented in Figure 2.

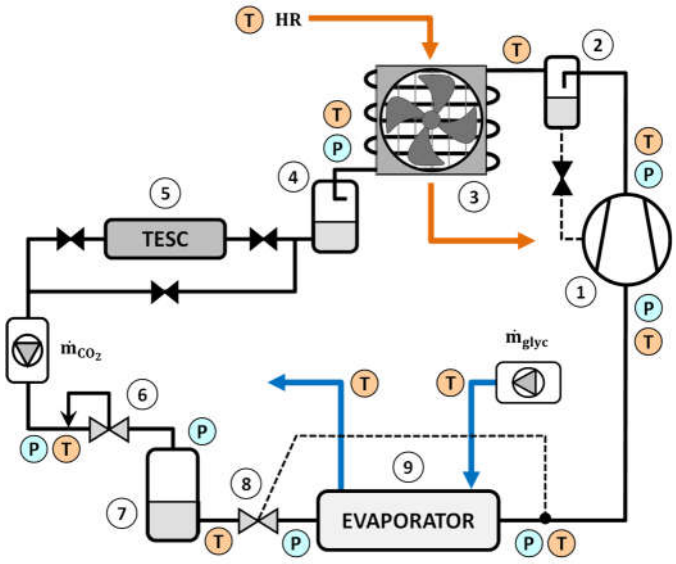

Figure 2 – Schematic diagram of the transcritical refrigeration system.

As Figure 2 shows, the transcritical cycle is composed by a hermetic compressor (1) with a cubic capacity of 1.1 cm^3 and a nominal rotation speed at 50 Hz of 2900 rpm; a coalescent filter (2) to separate the PAG lubricating oil from the compressor; an air finned-tube gas-cooler/condenser (3) with an inner-tube heat transfer area of 0.27 m^2 and an axial fan of 200 mm to reject the heat from the gas-cooler/condenser and to cool down the compressor; a small receiver of 0.2 litres (4) operating as liquid receiver in subcritical conditions; a thermoelectric subcooler (5) composed by 8 thermoelectric modules which description will be extended in Section 2.2; an electronic back-pressure valve (6) responsible for controlling the heat rejection pressure; an intermediate liquid receiver of 3.7 litres (7) to adjust the mass of refrigerant and to keep liquid conditions at the inner of the second expansion stage; an electronic thermostatic valve (8) dedicated to controlling a minimal useful superheating at the evaporator; and finally, a brazed-plate evaporator (9) with a heat transfer area of 0.576 m^2 using a mixture of water and ethylene-glycol (48.8% in mass) as secondary fluid. The refrigeration facility has a by-pass to isolate the thermoelectric subcooling in order to test the base-

cycle without subcooling. Moreover, the refrigerating plant has another by-pass not depicted in Figure 2 that isolates the back-pressure (6) and the liquid receiver (7) in subcritical conditions. The latter allows the effect of subcooling to be evaluated under subcritical conditions since the liquid receiver cancels out this effect.

To minimize the effect of heat exchange with the surroundings, all pipes and elements of the refrigeration facility are covered with foam with very low thermal conductivity, excluding the compressor and the gas-cooler/condenser.

During tests, the secondary fluid used in the refrigerating facility was prepared by an ad-hoc external system. The water-ethylene-glycol mixture was heated by a 1500W resistor controlled by a PID controller in a close loop. The volumetric flow was controlled by a recirculation pump and a metering valve. The entire experimental test bench was kept inside a climatic chamber during tests to maintain uniform ambient conditions. This air was used in the gas-cooler/condenser and also to cool down the thermoelectric modules as it will be described in Section 3.2.

3.2 Thermoelectric subcooler

The thermoelectric subcooling system consists of 4 blocks connected in series with 2 thermoelectric modules each (8 in total) as presents Figure 3.

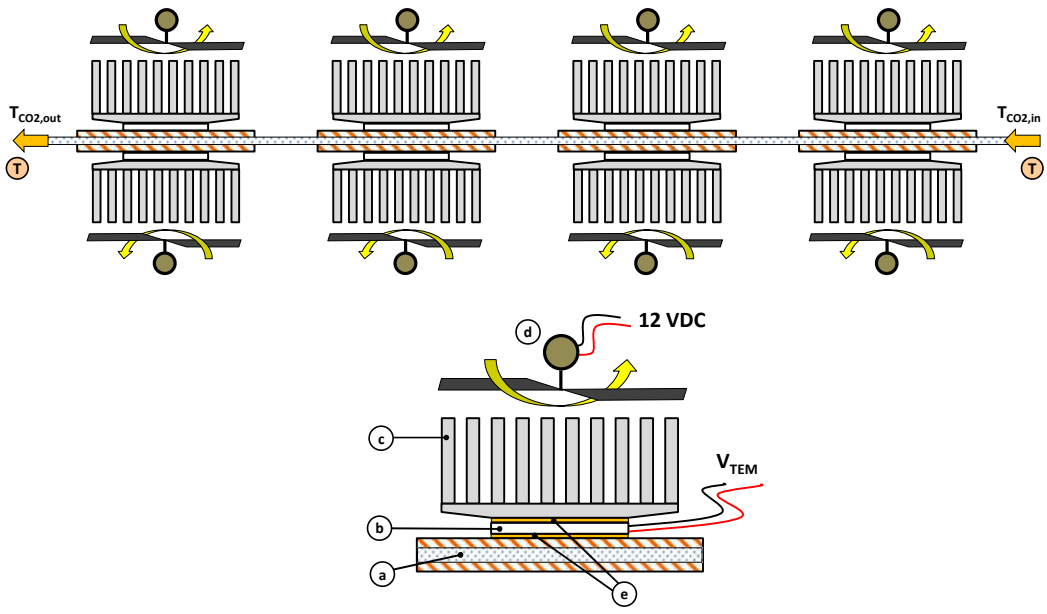

Figure 3 – Composition of the thermoelectric subcooling system and a detailed representation of a block.

Each block is assembled as Figure 3 depicts: A subcooler (a) made from a drilled block of pure copper with dimensions 60 x 74 x 10 mm and an inner surface of $3.56 \cdot 10^{-3}$ m^2; two thermoelectric modules (TEMs) (b) model RC12-8 from Marlow® industries placed conveniently centred over the subcooler surfaces; two

aluminium finned-sink (c) with 35 fins and a total external surface of 0.16 m^2; and finally, two axial fans of 80 mm of diameter each (d) with a nominal voltage and power consumption of 12 VDC and 1.4 W, respectively. The hot side of the TEMs is attached to the finned sink while the cold side is placed on the cooper blocks. All interfaces present a silicone thermal grease (e) with an average thermal conductivity of 5 $W \cdot m^{-1} \cdot K^{-1}$ to minimize the thermal contact resistance.

Each block is clamped with four screws installed in the finned sinks ensuring a tightening torque of 1 N·m with a torque wrench. Similarly to the refrigerating facility, the thermoelectric units are covered with foam to minimize heat exchange with their surroundings. Figure 4 shows the real aspect of the thermoelectric units installed in the refrigerating facility.

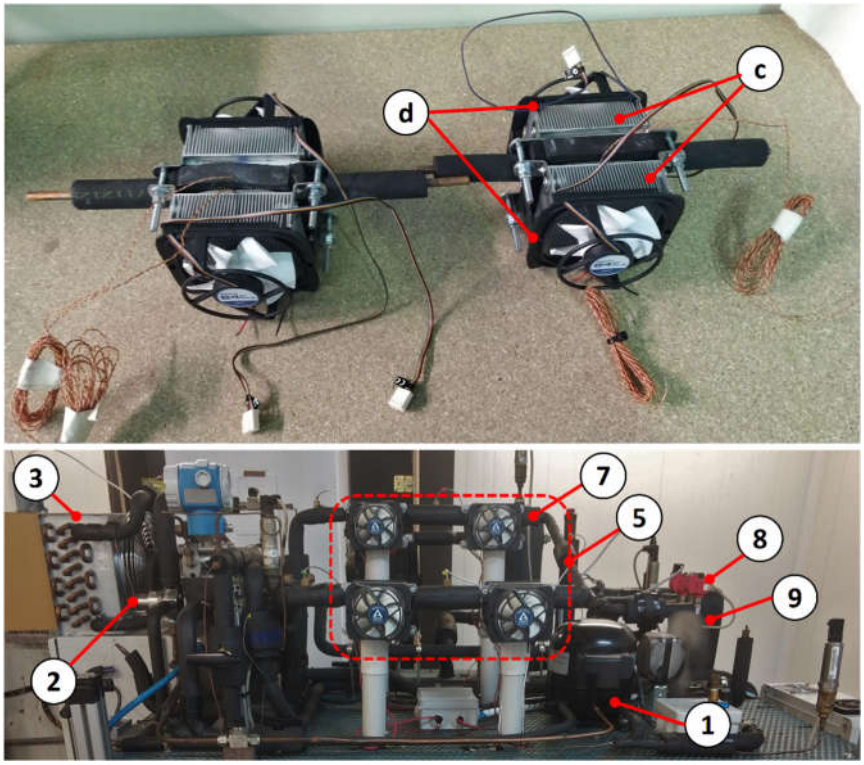

Figure 4 – Thermoelectric units and refrigerating facility equipped with the thermoelectric subcooling system.

TEMs are connected electrically in parallel to a power supply with a maximum power of 600W, 50 mV pp of ripple and 5 mV RMS of noise.

3.3 Measurement elements

The refrigerating facility is fully monitored with different measurement elements as detailed in Figure 2. Temperatures are measured with T-type thermocouples with an accuracy of ±0.5K according to UNE-EN 60584-1:2013; pressures are measured with pressure gauges with different ranges (0-160bar, 0-100bar and 0-60bar) and accuracy of ±0.5% of the spam; the mass flow rate of CO_2 and the water-ethylene-glycol

mixture are registered by two Coriolis mass flowmeters with an accuracy of ±0.5% of reading; electrical power is obtained with a power meter with an accuracy of ±0.5% of reading; and finally, the ambient temperature and the relative humidity are registered by a hygrometer with an accuracy of ±2.0% HR and ±0.2°C.

The thermoelectric subcooling system described in Figure 3 has also a digital multimeter to measure the voltage supplied to TEMs with an accuracy of ±0.05% of reading, and a current clamp meter for the current consumption of the TEMs with an accuracy of ±0.5% of reading.

All data were acquired by a data acquisition system (DAQ) with a registered time of 10 seconds for a minimum 15-minute stationary period. The information from the DAQ was recorded by a personal computer, and the thermophysical properties of the refrigerants and secondary fluids were calculated by RefProp v.10 [29] and SecCool v1.33 [30] software.

4 Test methodology

4.1 Reference variables

To determine the effect of using a TESC in a transcritical refrigerating plant, a series of variables were taken as a reference to define the operating conditions of the plant. The evaporating level (T_O) was maintained to -10ºC that is typically used in commercial refrigeration; the heat rejection conditions (temperature and relative humidity) were established according to ISO 23953-2 class III (25ºC; 60%) and class IV (30ºC; 55%); the useful superheating degree (SH) was fixed to 4K in all tests; and finally, the water-glycol mass flow rate ($\dot{m}_{glyc}$) was also maintained to 100 kg/h. Table 1 summarizes the average values of the reference parameters including their standard deviations during all tests.

Table 1 – Reference parameters.

UNE Conditions	T_{amb} (°C)	RH_{amb} (%)	T_O (°C)	$\dot{m}_{glyc}$ (kg/h)	SH (K)
Class III	25.1 ± 0.1	57.6 ± 1.6	-10.0 ± 0.1	100.7 ± 1.1	3.7 ± 0.1
Class VI	30.1 ± 0.1	54.8 ± 0.3	-10.1 ± 0.1	100.0 ± 1.2	4.0 ± 0.1

Since the whole experimental test bench was kept inside the climatic chamber to maintain uniform ambient conditions, the heat rejection conditions were equal for the gas-cooler/condenser and the TESC system.

4.2 Test procedure

Firstly, the refrigerating facility was tested without the TESC system to determine the optimum operating conditions. To achieve this, the operating conditions were defined with the parameters of Table 1 and the heat rejection pressure (P_{GC}) was varied from 95 bar to the minimum pressure corresponding to a liquid

receiver pressure equal to the critical pressure (73.8 bar). This limit was set to maintain stable operation in the refrigeration facility.

Once the optimum was identified, the TESC is added and the refrigerating plant was tested varying the voltage supplied to the thermoelectric modules and maintaining the same operating conditions stated before. In this case, the heat rejection pressure was fixed to different values near the base cycle optimum pressure. The voltage of the axial fans was fixed to 12 VDC in all tests.

4.3 Experimental data validation

The good agreement between the data obtained from the refrigerant and the secondary fluid is compared in Figure 5 using the cooling capacity ($\dot{Q}_O$) as reference. Eq. 5 and 6 were used to calculate the cooling capacity with CO_2 and the water-glycol mixture, respectively.

$$\dot{\mathbf{Q}}_{\mathbf{O.CO2}} = \dot{\mathbf{m}}_{\mathbf{CO2}} \cdot \left(\mathbf{h}_{\mathbf{O,CO2,out}} - \mathbf{h}_{\mathbf{O,CO2,in}}\right) \tag{5}$$

$$\dot{\mathbf{Q}}_{\mathbf{O.glyc}} = \dot{\mathbf{m}}_{\mathbf{glyc}} \cdot \mathbf{c}_{\mathbf{P,glyc}} \cdot \left(\mathbf{T}_{\mathbf{glyc,in}} - \mathbf{T}_{\mathbf{glyc,out}}\right) \tag{6}$$

Figure 5 shows the average values of cooling capacities at the evaporator working with and without the subcooling system. The standard deviation of the measured variables are presented as error bars.

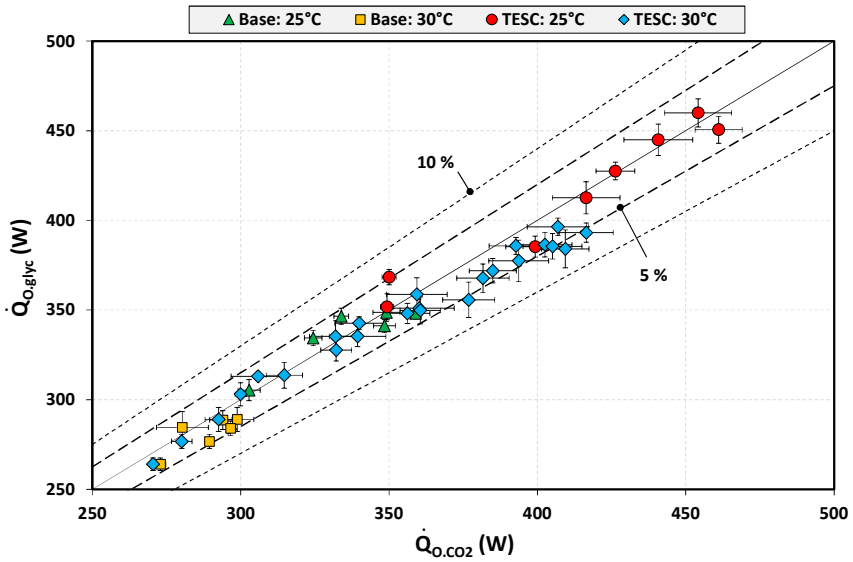

Figure 5 – Data validation with the measuring data at the evaporator.

By considering the data presented in Figure 5, the maximum difference of cooling capacity between the secondary fluid and the refrigerant is 6.6% so it can be asserted that the measurement system is operating properly and the values obtained from the experimental tests are reliable.

5 Experimental analysis

5.1 Base cycle

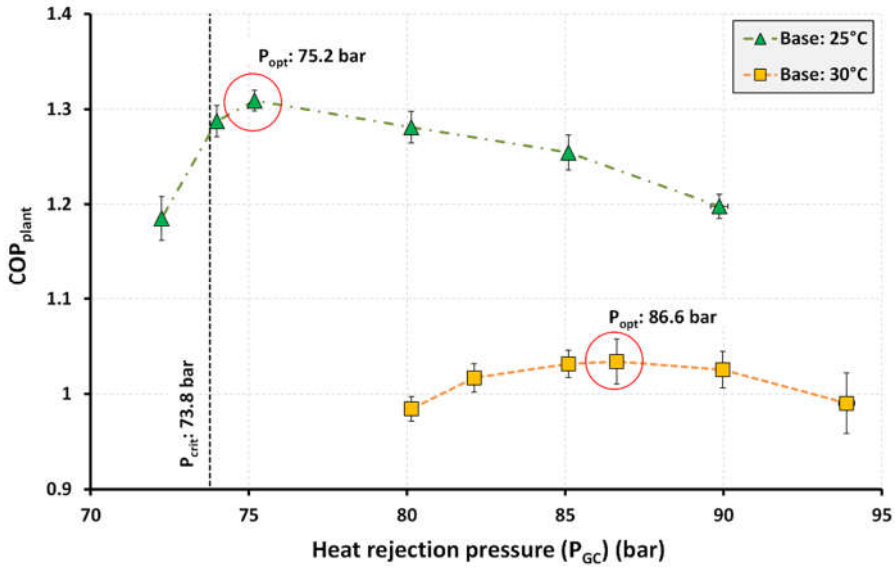

Figure 6 – Measured values of COP for the base cycle at the evaporating temperature of -10ºC.

As Figure 6 shows, tests were conducted at several heat rejection pressures from 95 bar to a minimal pressure which ensures a pressure in the liquid receiver (7) above the critical one (73.8 bar): 80 bar for 30ºC and 72 bar for 25ºC. This limitation is made to assess the stability of the cycle according to the behaviour described by Cabello *et al.* in [31]. Once these pressures are determined, a polynomial equation COP vs. Pressure was determined by the least-square best-fit method obtaining an optimal pressure value. Finally, the theoretical optimal pressure was corroborated experimentally with new tests equal and near this value.

As it can be seen in Figure 6, the optimum pressure ($P_{GC,opt}$) depends on the climatic condition, the higher the heat rejection temperature, the higher is the optimum heat rejection pressure. This behaviour corresponds with the experimental results reported by [31] and [32] which predict that the COP drops sharply near the pseudocritical temperature, especially in subcritical conditions near the critical temperature.

Table 2 summarizes the average value and the standard deviation of different parameters from the base cycle at the optimum operating conditions (maximum COP). These parameters include the optimum heat rejection pressure, the maximum COP of the refrigeration plant, the cooling capacity, the power consumption of the facility and the pressure level of the liquid receiver at the optimum conditions. These values will be taken into account in the following sections to compare with the TESC results.

Table 2 – Relevant parameters at the optimum operating conditions for the base cycle.

T_{amb} (°C)	T_O (°C)	$P_{GC.opt}$ (bar)	$COP_{plant.opt}$	$\dot{Q}_{O.plant.opt}$ (W)	$\dot{W}_{CO2.opt}$ (W)	$P_{LR.opt}$ (bar)
25.0 ± 0.1	-10.0 ± 0.1	75.2 ± 0.0	1.31 ± 0.01	348.0 ± 2.9	265.7 ± 0.3	65.8 ± 0.1
30.1 ± 0.0	-10.0 ± 0.1	86.6 ± 0.1	1.03 ± 0.02	289.0 ± 6.7	279.5 ± 0.5	68.5 ± 0.1

5.2 Thermoelectric subcooling cycle

To analyse the impact of using the TESC system, the refrigerating plant has been tested at the same operating conditions stated before while the voltage supply to the TEMs varies from 0 to 10 VDC. Concerning the heat rejection pressure, the results obtained by Astrain *et al.* in transcritical conditions revealed that the optimum pressure using a TESC system was lower than the base cycle one, being 75 bar at an ambient temperature of 25ºC, and 79 bar for 30ºC [21]. Accordingly, in this study, the heat rejection pressure has being maintained to 75 and 80 bar for the climate conditions of 25 and 30ºC, respectively. Additionally, to analyse the effect of the heat rejection pressure over the TESC operation, the pressures of 83 and 86 bar have been included in the experimental analysis at 30ºC.

The following subsections show how the subcooling effect introduced by the TESC varies the parameters of cooling capacity, power consumption, COP and subcooling effect. Each subsection presents a figure with the average value of the measured or calculated data including the error bars calculated by the Moffat method for indirect measurements [33]. It is important to notice that in all cases, the TEM voltage of 0 VDC corresponds to the base cycle without the TESC system

5.2.1 Cooling capacity

The effect of the TESC system on the cooling capacity is presented in Figure 7 as a function of the voltage supplied to the TEMs at the ambient temperatures of 25 and 30ºC. Moreover, Figure 7 includes the results obtained at the three heat rejection pressures analysed with ambient temperature of 30ºC.

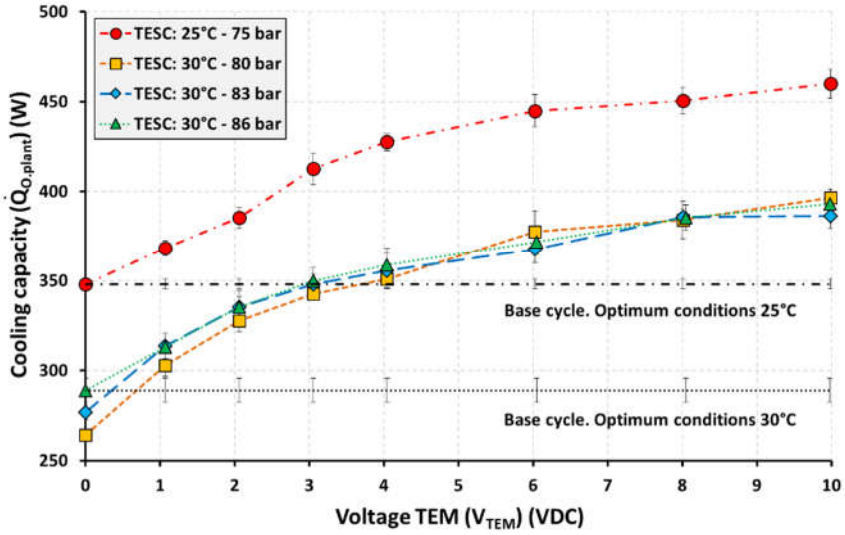

Figure 7 – Cooling capacity of the refrigerating plant at different TEM voltage supplies.

As it can be observed in Figure 7, the use of the TESC system always enhances the cooling capacity of the refrigerating plant as the cooling capacity is defined by the sum of the base cycle capacity and the cooling effect introduced by the thermoelectric modules (Eq. 1). Although increments of capacity up to 32.2% at 25ºC and up to 50.2% at 30ºC can be obtained when the voltage supply is 10 VDC, as section 5.2.4 includes, these working points may not be interesting for the optimal operation of the refrigeration plant. Notwithstanding, the use of the TESC system allows easy increment on the capacity of the refrigerating plant by varying the voltage supply of the thermoelectric modules. This minimizes the cost and the complexity of the refrigerating plant, extending its useful range to cover increments of the cooling demand.

Regarding the effect of the heat rejection pressure at 30ºC, Figure 7 presents a slight increment of cooling capacity at heat rejection pressures of 83 and 86 bar. This increment is appreciable for voltage supplies lower than 4 VDC but not for higher ones. The main effect of these results on the COP of the plant will be discussed later.

5.2.2 Power consumption

The power consumption of the refrigerating plant is defined by Eq. 2 as the sum of the power consumed by the compressor and the power consumed by the TESC system including the fans of the heat-sinks. Figure 8 presents the values obtained from the experimental tests at different voltage supplies.

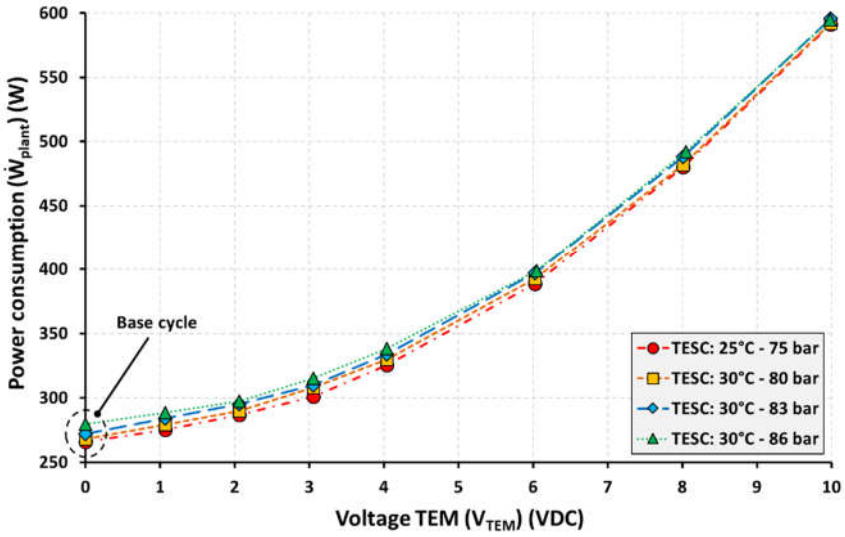

Figure 8 – Power consumption of the refrigerating plant at different TEM voltage supplies.

The measured values of Figure 8 highlight the increase in consumed power by the refrigerating plant as the voltage supply increases regardless of the operating conditions. As is evident from tests, this increase is especially quadratic at high voltage supplies where the thermoelectric modules perform worse due to the high-temperature difference between their faces [34]. This behaviour is detailed in Figure 9 using the

experimental data from tests at 30ºC and 80 bar as an example. Accordingly, the power consumed in the experimental plant is split into each active element: compressor, thermoelectric modules and heat-sink fans. It should be underlined that the power consumed by the DC supply has not been considered, since it must be optimized at the optimum operating conditions which this work aims to find.

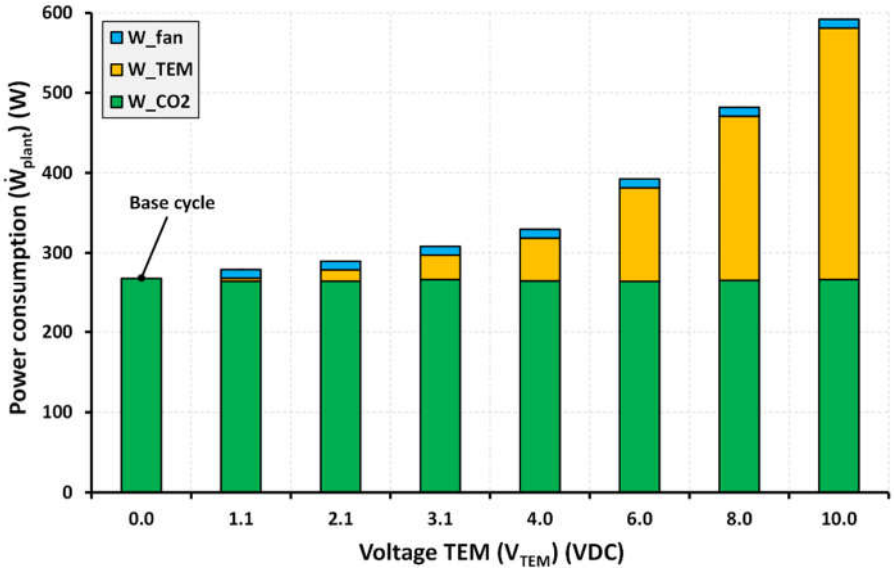

Figure 9 – Detailed power consumption of the refrigerating plant for 30ºC and 80 bar.

As Figure 9 shows, for fixed evaporating temperature and heat rejection conditions (temperature and pressure), the compressor power consumption ($\dot{W}_{CO2}$) remains constant because the pressure levels of the CO_2 vapour compression cycle are constant as well as the temperature at the compressor suction port. Regarding the power consumed by the thermoelectric modules ($\dot{W}_{TEM}$), it increases smoothly at low voltage supplies (up to 4 VDC) but rises sharply at high voltages due to the deterioration of their performance. At these values, the power consumed by the TESC becomes even higher than that of the CO_2 compressor. Finally, the power consumed by the heat-sink fans ($\dot{W}_{FAN}$) is constant (approx. 11 W) and represents an important part of the TESC power consumption especially at low voltages. According to Aranguren *et al.*, this power is necessary but its minimization is urgent to improve the performance of the system [35].

5.2.3 COP

Regarding the COP of the refrigerating plant, it has been calculated with Eq. 3 and taking into account all active components of the system, namely the compressor, the TEMs and the heat-sink fans. Figure 10 presents the values of COP at both climatic conditions analysed including the different heat rejection pressures.

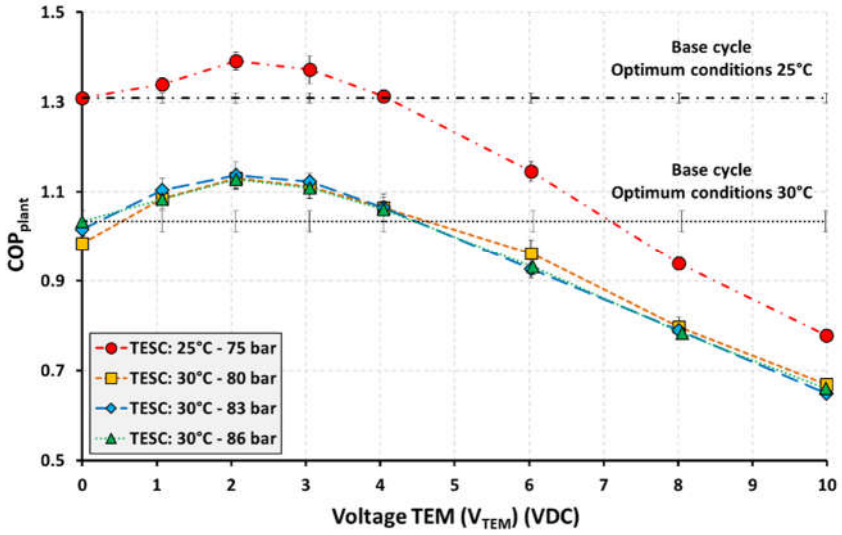

Figure 10 – COP of the refrigerating plant at different TEM voltage supplies.

From the results depicted in Figure 10, there are different points that would seem to be particularly noteworthy. The first is the positive effect of the TESC system at voltages lower than 4 VDC and the negative effect for higher voltages. This is because of the penalization that suffers the COP of the TEMs at high voltage supplies due to the higher power consumption of these, as detailes Figure 9. Figure 11 presents the COP of the refrigerating plant (COP_{plant}), the TESC system (COP_{TESC}) and the base cycle (COP_{CO2}) at 30ºC and 80 bar. From this Figure is evident that the COP_{plant} is higher than the COP_{CO2} only when the condition $COP_{TESC} > COP_{CO2}$ is achieved, so higher values of COP_{plant} are only possible if COP_{TESC} is maximized by minimizing the TESC power consumption (fans and TEMs).

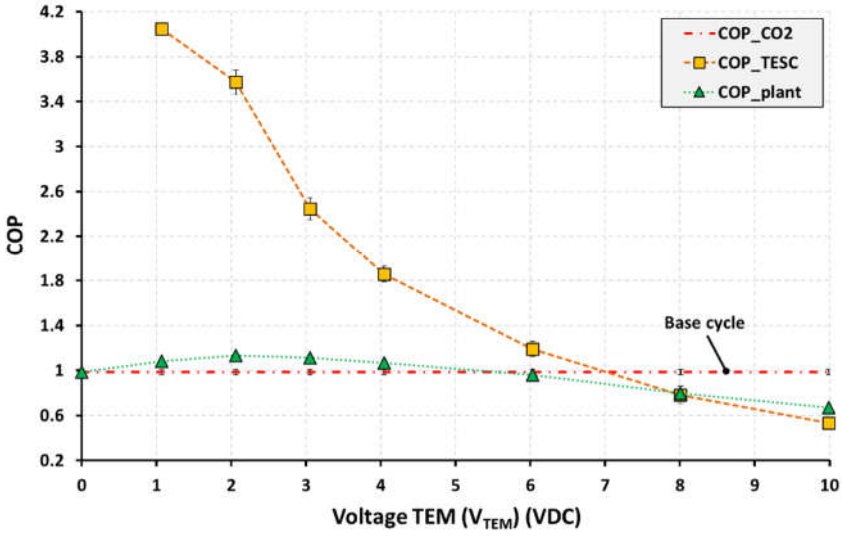

Figure 11 – Detailed COP of the refrigerating plant, the base cycle and the TESC system for 30ºC and 80 bar.

Another important point is the existence of an optimum voltage supply that maximizes the COP of the refrigerating plant (COP_{plant}), which value is around 2 VDC according to the experimental results at the two climatic conditions analysed in this work. Moreover, this value is coincident with those theoretical voltage calculated previously by Astrain *et al.* [21].

Finally, at the optimal voltage of TEMs, the increments of COP concerning the base cycle at each particular pressure were +14.9% at 80 bar, +11.7% at 83 bar, and +9.1% at 86 bar. These results show that the positive effect of the TESC depends on the heat rejection pressure especially near the pseudocritical region where the COP of the base cycle drops quickly (Figure 6). However, for the purpose of ensuring a fair comparison between the base cycle and the TESC cycle, COP should be compare at the optimal operating conditions in both arrangements. Thus, section 5.2.5 compares the experimental results of both arrangements at the optimum operating conditions.

5.2.4 Subcooling effect

The subcooling effect (ΔT_{SUB}) is defined by Eq. (7) as the difference between the gas-cooler outlet temperature ($T_{GC,out}$) and the temperature at the inlet of the back-pressure valve ($T_{BP,in}$):

$$\Delta \mathbf{T_{SUB}} = \mathbf{T_{GC.out}} - \mathbf{T_{BP,in}} \tag{7}$$

Figure 12 presents the subcooling degree introduced by the TESC system at different voltage supplies. The subcooling degree rises linearly with the voltage supply up to 4 VDC, however for voltages greater than 4 VDC this increment is not linear due to the performance deterioration of the thermoelectric modules. The main consequence of this trend is the cooling capacity variation presented in Figure 7.

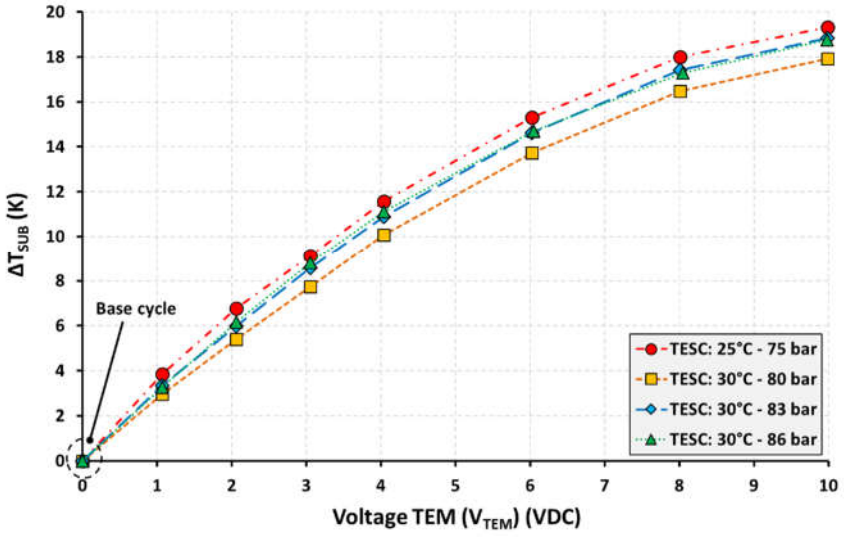

Figure 12 – Subcooling degree introduced by the TESC system at different TEM voltage supplies.

Focusing on the subcooling effect at 30ºC, it can be observed how the subcooling degree introduced by the TESC system increases as the heat rejection pressure increases. This effect is caused by the abrupt change that thermophysical properties suffer near the pseudocritical temperature, especially the isobaric specific heat which increment minimizes the subcooling effect. Table 3 compares, at the same heat rejection temperature and TEM voltage supply, the electrical power consumed by the TESC system (TEM and fans) ($\dot{W}_{TESC}$), the average inlet temperature to the TESC system ($T_{TESC,in}$), the subcooling effect (ΔT_{SUB}), the cooling effect of the thermoelectric subcooler ($\dot{Q}_{O.TESC}$), the COP of TESC (COP_{TESC}) and the pseudocritical temperature (T_{pseudo}), the latter obtained with the expression adjusted by Liao and Zhao [36].

Table 3 – Temperatures and subcooling effect in the TESC system at 30ºC and 2 VDC.

P_{GC} (bar)	T_{amb} (°C)	$\dot{W}_{TESC}$ (W)	$T_{TESC,in}$ (°C)	T_{pseudo} (°C)	ΔT_{SUB} (K)	$\dot{Q}_{O.TESC}$ (W)	COP_{TESC}
80.2	30.1	24.9	34.1	34.8	5.4	88.9	3.57
83.3	30.1	24.4	33.0	36.5	6.0	56.9	2.33
86.1	30.2	24.0	32.7	37.9	6.2	52.3	2.18

From Table 3 is evident that the nearer the $T_{TESC,in}$ is to pseudocritical temperature, the lower subcooling degree introduces the thermoelectric subcooler due to increment of the isobaric specific heat. Moreover, near the pseudocritical temperature, the cooling effect and the COP of the TESC system increase due to the improvement of the CO_2 heat transfer coefficient [36] which minimizes the thermal resistances involved in the TESC, and consequently, the temperature difference between the cold and the hot side of the thermoelectric modules.

As a consequence of the subcooling introduced by the TESC system, the pressure and the temperature of the liquid receiver decrease, increasing at the same time the liquid density of the refrigerant stored in it. The main consequence of this density variation is the reduction of the useful liquid level in the liquid receiver so it is important to make sure that there is enough refrigerant mass charge in the liquid receiver to feed properly the second expansion device. Additionally, the temperature reduction on the liquid receiver would mean higher thermal insulation for this component to avoid thermal loads from ambient.

5.2.5 Summary of the experimental results

The results obtained at the optimum conditions for both analysed cycles are summarized in Table 4, where the effect of the TESC system has been highlighted including the increments of the main variables with regard to the base cycle also operating at the optimum conditions. Eq. (8) has been used to determine the increments of COP ($COP_{plant.opt}$), cooling capacity ($\dot{Q}_{O.plant.opt}$) and power consumption ($\dot{W}_{plant.opt}$), using "X" as the analysed variable. Eq. (9) allows determining the pressure increments for the optimal heat rejection pressure ($P_{GC.opt}$) and the liquid receiver pressure ($P_{LR.opt}$).

$$\Delta X = 100 \cdot \frac{X_{TESC} - X_{Base}}{X_{Base}} \quad (8)$$

$$\Delta P = P_{TESC} - P_{Base} \quad (9)$$

Table 4 – Results of the refrigerating plant under optimal operating conditions (maximum COP).

Cycle	T_{amb} (°C)	$V_{TEM.opt}$ (VDC)	$COP_{plant.opt}$	$\dot{Q}_{O.plant.opt}$ (W)	$\dot{W}_{plant.opt}$ (W)	$P_{GC.opt}$ (bar)	$P_{LR.opt}$ (bar)
Base	25.0 ± 0.1	-	1.31 ± 0.01	348.0 ± 2.9	265.7 ± 0.3	75.2 ± 0.0	65.8 ± 0.1
TESC	25.2 ± 0.1	2.06 ± 0.01	1.39 ± 0.02	385.3 ± 5.8	286.8 ± 0.6	75.3 ± 0.0	57.5 ± 0.1
	Increment (ΔX, ΔP)		+6.3 %	+10.7 %	+8.0 %	+0.1 bar	-8.3 bar
Base	30.1 ± 0.0	-	1.03 ± 0.02	289.0 ± 6.7	279.5 ± 0.5	86.6 ± 0.1	68.5 ± 0.1
TESC	30.1 ± 0.0	2.06 ± 0.01	1.14 ± 0.03	335.3 ± 8.9	295.1 ± 1.1	83.3 ± 0.1	62.8 ± 0.1
	Increment (ΔX, ΔP)		+9.9 %	+16.0 %	+5.6 %	-3.3 bar	-5.7 bar

According to Table 4, the use of the thermoelectric subcooling system at the optimum operating conditions provides an increment of the refrigerating plant COP around +6.3% at 25ºC and +9.9% at 30ºC. Therefore, the improvement of the global COP becomes higher as higher is the ambient temperature, which is very common when subcooling is applied [37]. Similarly, the optimum pressures with the TESC system are lower or equal than those of the base cycle, especially at the ambient temperature of 30ºC where a reduction up to 3.3 bar is recorded.

Regarding the cooling capacity, the presence of the thermoelectric subcooler improves the capacity of the refrigerating plant up to +10.7% at 25ºC and up to +16.0% at 30ºC, which extends the operating range of the refrigerating plant and makes easy its regulation. This effect is crucial for low-medium applications with no variable-speed compressors when they need to provide additional cooling in pull-down process.

Finally, the presence of an active subcooling entails an increment of the power consumption by refrigerating plant. However, this increment is relatively low comparing with other active subcooling systems as will be discussed in the next section. Notwithstanding, it is worth to mention that this increment could be minimized by optimizing the voltage supply of each thermoelectric module or by minimizing auxiliary power consumption.

6 Comparative assessment

Since the IHX and the dedicated mechanical subcooling (DMS) are other suitable subcooling techniques for transcritical cycles, it is interesting to compare them to determine the improvement degree at similar operating conditions. To do that, the experimental results determined by Sanchez *et al.* have been taken as reference using an IHX and an R600a DMS in a small capacity plant [38]. The comparison considers an inlet temperature of 30ºC for the secondary fluid in the gas-cooler, although the fluid used in [38] is water instead of air. Accordingly, the approach temperature for the DMS and IHX tests are better than the TESC tests (~3K lower) so the results of these arrangements are slightly better than expected. Moreover, the auxiliary power consumption to pump the water through the condenser of the DMS unit has not been

considered in the experimental tests of [38], so to ensure a fair comparison, the auxiliary power consumed by fans of the TESC has been removed and similar operating conditions of TEMs have been assumed.

Table 5 summarizes the effect of all subcooling systems expressed as increment regarding the base cycle. The non-optimized dedicated mechanical subcooling corresponds to the experimental tests while the optimized one is the optimized cycle with a computational model also described in [38].

Table 5 – Effect of different subcooling systems on the base cycle at -10ºC and 30ºC at the optimum operating condition

Subcooling technique	$\Delta P_{GC.opt}$ (bar)	ΔCOP_{plant} (%)	$\Delta \dot{Q}_{O.plant}$ (%)	$\Delta \dot{W}_{plant}$ (%)
IHX	-2.0	+3.7	+3.3	-0.4
DMS with R600a	-2.0	+12.3	+32.3	+17.9
TESC (without auxiliary consumption)	-3.3	+14.1	+16.0	+1.7
DMS with R600a (optimized)	-2.6	+17.7	+32.6	+12.7

According to Table 5, the results provided by the TESC system without auxiliary consumption are better than those obtained by the IHX installed at the exit of the gas-cooler or the experimental DMS with R600a. Moreover, the results from TESC are quite similar to an optimized R600a DMS system in terms of COP and optimal heat rejection pressure, but with a reduced impact over the global power consumption of the refrigerating plant. Furthermore, this original system provides an almost linear capacity regulation easily adjustable by varying the voltage supply, with high robustness and compactness, low-complexity, low-cost and absence of additional refrigerants.

7 Conclusions

This work experimentally evaluates the benefits of using a thermoelectric subcooler system (TESC) installed in a CO_2 transcritical refrigeration plant at the exit of the gas-cooler. The experimental test campaign has been performed at two climatic conditions: 25ºC/60% and 30ºC/55% for different heat rejection conditions, and an evaporative level of -10ºC, a common level in commercial refrigeration. The voltage supply to the thermoelectric modules has been varied up to 10 VDC with a fixed voltage supply for the heat-sink fans installed on the hot-face of the modules.

From tests, it has been demonstrated that thermoelectric subcooling is an effective method to increase the cooling capacity of the refrigerating plant with an almost linear capacity regulation, easily adjustable by varying the voltage supply. Thus, at the optimum voltage supply of 2 VDC, the results provide increments of +10.7% at 25ºC and +16.0% at 30ºC.

Regarding the COP, the experimental results have demonstrated the existence of an optimum voltage around 2 VDC that maximizes the COP of the refrigerating plant according to the theoretical analysis previously published by other authors. At this optimum voltage, the increments with regard to the optimum

values of the base cycle without subcooling are +6.3% at 25ºC and 75.3 bar, and +9.9% at 30ºC and 83.3 bar. Test also revealed a reduction on the optimum pressure of 3.3 bar at 30ºC.

Finally, a comparison between the TESC and the subcooling methods of IHX and DMS evidences that TESC provides better results than the IHX and similar results to the mechanical subcooling system in terms of COP with lower energy penalizations. Therefore, thermoelectric subcooler reports substantial improvements easily adjustable, with high robustness and compactness, low-cost and absence of additional refrigerants.

Future works based on the results obtained will be addressed on the optimization of the energy consumption of the TESC system by optimizing the voltage supply of each thermoelectric block.

Acknowledgements

The authors would like to acknowledge the support of the Spanish Ministry of Science, Innovation and Universities, and European Regional Development Fund, for the funding under the RTI2018-093501-B-C21 and RTI2018-093501-B-C22 research projects.

References

[1] International Institute of Refrigeration. *35th Informatory Note of Refrigeration Technologies. The impact of the refrigeration sector on climate change*. IIR, France (2017). https://iifiir.org/fr/fridoc/141135

[2] International Institute of Refrigeration. *29th Informatory Note of Refrigeration Technologies. The role of refrigeration in the Global Economy*. IIR, France (2015). https://iifiir.org/en/fridoc/138763

[3] Lorentzen G. *The use of natural refrigerants: a complete solution to the CFC/HCFC predicament*. International J. Refrigeration 18 (1995) 190–7. https://doi.org/10.1016/0140-7007(94)00001-E

[4] Lorentzen G., Pettersen J. *A new, efficient and environmentally benign system for car air-conditioning*. International J. Refrigeration 16 (1993) 4–12. https://doi.org/10.1016/0140-7007(93)90014-Y

[5] Dai B., Li M., Ma Y. *Thermodynamic analysis of carbon dioxide blends with low GWP (global warming potential) working fluids-based transcritical Rankine cycles for low-grade heat energy recovery*. Energy 64 (2014) 942–52. https://doi.org/10.1016/j.energy.2013.11.019

[6] Robinson D.M., Groll E.A. *Efficiencies of transcritical CO_2 cycles with and without an expansion turbine*. International J. Refrigeration 21 (1998) 577–589. https://doi.org/10.1016/S0140-7007(98)00024-3

[7] Kim Man-Hoe, Petersen J., Bullard C.W. *Fundamental process and system design issues in CO_2 vapor compression systems*. Progress in Energy and Combustion Science 30, 2 (2004) 119–174. https://doi.org/10.1016/j.pecs.2003.09.002

[8] Sánchez D., Patiño J., Llopis R., Cabello R., Torrella E., Vicente Fuentes F. *New positions for an internal heat exchanger in a CO_2 supercritical refrigeration plant. Experimental analysis and energetic evaluation*. Applied Thermal Engineering 63, 1 (2014) 129–139. https://doi.org/10.1016/j.applthermaleng.2013.10.061

[9] Torrella E., Sánchez D., Llopis R., Cabello R. *Energetic evaluation of an internal heat exchanger in a CO_2 transcritical refrigeration plant using experimental data*. International J Refrigeration 34 (2011) 40–49. https://doi.org/10.1016/j.ijrefrig.2010.07.006

[10] Sarkar J., Agrawal N. *Performance optimization of transcritical CO_2 cycle with parallel compression economization*. International J. Thermal Sciences 49, 5 (2010) 838–843. https://doi.org/10.1016/j.ijthermalsci.2009.12.001

[11] Lucas C., Koehler J. *Experimental investigation of the COP improvement of a refrigeration cycle by use of an ejector*. International J. Refrigeration 35 (2012) 1595–603. https://doi.org/10.1016/j.ijrefrig.2012.05.010

[12] Zhang B., Zhao D., Zhao Y., Ji H., Chen L., Liu L. *Comparative Analysis of Typical Improvement Methods in Transcritical Carbon Dioxide Refrigeration Cycle*. Procedia Engineering 205 (2017) 1207–1214. https://doi.org/10.1016/j.proeng.2017.10.355

[13] Catalán-Gil J., Nebot-Andrés L., Sánchez D., Llopis R., Cabello R., Calleja-Anta D. *Improvements in CO_2 Booster architectures with different economizer arrangements*. Energies 13 (5) (2020) 1271. https://doi.org/10.3390/en13051271

[14] Nebot-Andrés L., Catalán-Gil J., Sánchez D., Calleja-Anta D., Cabello R., Llopis R. *Experimental determination of the optimum working conditions of a transcritical CO_2 refrigeration plant with integrated mechanical subcooling*. International J. Refrigeration 113 (2020) 266–275. https://doi.org/10.1016/j.ijrefrig.2020.02.012

[15] Catalán-Gil J., Llopis R., Sánchez D., Nebot-Andrés L., Cabello R. *Experimental evaluation of the desuperheater influence in a CO2 booster refrigeration facility*. Applied Thermal Engineering 168, 5 (2020) 114785. https://doi.org/10.1016/j.applthermaleng.2019.114785

[16] Rowe DM. *Handbook of Thermoelectrics*. CRC New York 16 (1995) 1251–1256. https://doi.org/10.1016/S0960-1481(98)00512-6

[17] Jamali S., Yari M., Mohammadkhani F. *Performance improvement of a transcritical CO_2 refrigeration cycle using two-stage thermoelectric modules in sub-cooler and gas cooler*. International J. Refrigeration 74 (2017) 103–113. https://doi.org/10.1016/j.ijrefrig.2016.10.007

[18] Dai B., Liu S., Zhu K., Sun Z., Ma Y. *Thermodynamic performance evaluation of transcritical carbon dioxide refrigeration cycle integrated with thermoelectric subcooler and expander*. Energy 122 (2017) 787–800. https://doi.org/10.1016/j.energy.2017.01.029

[19] Winkler J., Aute V., Yang B., Radermacher R. *potential benefits of thermoelectric elements used with air-cooled heat exchangers*. International Refrigeration and Air Conditioning Conference (2006). Paper 813. http://docs.lib.purdue.edu/iracc/813

[20] Sarkar J. *Performance optimization of transcritical CO_2 refrigeration cycle with thermoelectric subcooler*. International J. Energy Research 37 (2013) 121–128. https://doi.org/10.1002/er.1879

[21] Astrain D., Merino A., Catalán L., Aranguren P., Araiz M., Sánchez D., Cabello R., Llopis R. *Improvements in the cooling capacity and the COP of a transcritical CO_2 refrigeration plant operating with a thermoelectric subcooling system*. Applied Thermal Engineering 155 (2019)110–122. https://doi.org/10.1016/j.applthermaleng.2019.03.123

[22] Schoenfeld J., Muehlbauer J., Hwang Y., Radermacher R. *Integration of a thermoelectric subcooler into a carbon dioxide transcritical vapor compression cycle* International Refrigeration and Air Conditioning Conference (2008). Paper 903. http://docs.lib.purdue.edu/iracc/903

[23] Schoenfeld J.M. *Integration of a thermoelectric subcooler into a carbon dioxide transcritical vapor compression cycle refrigeration system*. Master thesis (2008). https://drum.lib.umd.edu/handle/1903/8726

[24] Araiz M., Catalán L., Herrero O., Rodriguez A., Pérez M.G. *The Importance of the Assembly in Thermoelectric Generators*. Bringing Thermoelectricity into Reality. Chapter 7. IntechOpen (2018) http://dx.doi.org/10.5772/intechopen.75697

[25] Astrain D., Vián J.G., Martínez A., Rodríguez A. *Study of the influence of heat exchangers' thermal resistances on a thermoelectric generation system*. Energy 35 (2010) 602–610. https://doi.org/10.1016/j.energy.2009.10.031

[26] Cai Y., Liu D., Yang J-J., Wang Y., Zhao F-Y. *Optimization of Thermoelectric Cooling System for Application in CPU Cooler*. Energy Procedia 105 (2017) 1644–1650. https://doi.org/10.1016/j.egypro.2017.03.535

[27] Liu D., Cai Y., Zhao F.Y. *Optimal design of thermoelectric cooling system integrated heat pipes for electric devices*. Energy 128 (2017) 403–413. https://doi.org/10.1016/j.energy.2017.03.120

[28] Llopis R., Nebot-Andrés L., Sánchez D., Catalán-Gil J., Cabello R., *Subcooling methods for CO_2 refrigeration cycles: A review*. International J. Refrigeration 93 (2018) 85–107. https://doi.org/10.1016/j.ijrefrig.2018.06.010

[29] Lemmon E. W., Huber M. L., McLinden M. O., *Reference fluid thermodynamic and transport properties (REFPROP)*, NIST Standard Reference Database 23, v.9.1. National Institute of Standards 2013. Gaithersburg MD, USA.

[30] SecCool v.1.33 Properties. IPU Refrigeration and Energy Engineering (2007).

[31] Cabello R., Sánchez D., Llopis R., Torrella E., *Experimental evaluation of the energy efficiency of a CO_2 refrigerating plant working in transcritical conditions*. Applied Thermal Engineering 28 (2008) 1596–1604. https://doi.org/10.1016/j.applthermaleng.2007.10.026

[32] Sánchez D., Patiño J., Sanz-Kock C., Llopis R., Cabello R., Torrella E. *Energetic evaluation of a CO_2 refrigeration plant working in supercritical an subcritical conditions*. Applied Thermal Engineering 66, 1-2 (2014) 227–238. https://doi.org/10.1016/j.applthermaleng.2014.02.005

[33] Moffat R.J., *Describing the uncertainties in experimental results*, Experimental Thermal and Fluids Science, 1 (1988) pp. 3-17.

[34] Aranguren P., DiazDeGarayo S., Martínez A., Araiz M., Astrain D. *Heat pipes thermal performance for a reversible thermoelectric cooler-heat pump for a nZEB*. Energy and Buildings 187 (2019) 163–172. https://doi.org/10.1016/j.enbuild.2019.01.039

[35] Aranguren P., Araiz M., Astrain D. *Auxiliary consumption: A necessary energy that affects thermoelectric generation*. Applied Thermal Engineering 141 (2018) 990–999. https://doi.org/10.1016/j.applthermaleng.2018.06.042

[36] Liao S. M., Zhao T.S. *Measurements of heat transfer coefficients from supercritical carbon dioxide flowing in horizontal mini/micro channels.* Journal of Heat Transfer 124 (2002) 413-420.

[37] Sánchez D., Catalán-Gil J., Llopis R., Nebot-Andrés L., Cabello R., Torrella E., *Improvements in a CO_2 transcritical plant working with two different subcooling systems*. Refrigeration Science and Technology (2016) 1014 – 1022. http://dx.doi.org/10.18462/iir.gl.2016.1170

[38] Sánchez D., Catalán-Gil J., Cabello R., Calleja-Anta D., Llopis R., Nebot-Andrés L. *Experimental analysis and optimization of an R744 transcritical cycle working with a mechanical subcooling system*. Energies 13 (12) (2020) 3204. https://doi.org/10.3390/en13123204